Economic Geology
Vol. 97, 2002, pp. 1341–1346

AN EVALUATION OF FLUID INCLUSION MICROTHERMOMETRIC DATA FOR ORPIMENT-REALGAR-CALCITE-BARITE-GOLD MINERALIZATION AT THE BETZE AND CARLIN MINES, NEVADA

JOHN A. GROFF,† ANDREW R. CAMPBELL, AND DAVID I. NORMAN

New Mexico Institute of Mining and Technology, Dept. of Earth and Environmental Sciences, Socorro, New Mexico 87801

Abstract

Carlin-type deposits contain gold in association with main-stage quartz-pyrite-kaolinite mineralization and late-stage orpiment-realgar-calcite-barite mineralization. Fluid characteristics for main-stage mineralization are well documented by fluid inclusion and stable isotope studies on quartz. In contrast, fluid characteristics for late-stage mineralization are not well constrained because of large ranges in fluid inclusion microthermometric data. These ranges could represent real variations in fluids or be a result of the reequilibration of fluid inclusions.

Microthermometric analyses were conducted on fluid inclusions in samples of barite, calcite, realgar, and orpiment from the Betze and Carlin mines, Nevada. Petrographic studies of individual crystals and cleaved sections reveal that fluid inclusions in realgar and barite have negative crystal shapes, in contrast to elongate and rounded inclusions in orpiment and calcite. Point-count data document that one-phase liquid inclusions (type 1) are the dominant type in barite and realgar, relative to two-phase, vapor-poor inclusions (type 2) in calcite and orpiment. Type 2 inclusions in realgar and barite commonly reequilibrate (e.g., stretch) during analysis and exhibit ranges in homogenization temperatures (T_h) of 100º to 250ºC and 110º to 300ºC, respectively. In contrast, type 2 inclusions in orpiment and calcite have T_h of 108º to 182ºC, which could be repeated to within 1ºC. Based on these results, fluid inclusions in barite and realgar are most susceptible to reequilibration, with T_h of ~100º to 110ºC most representative. Fluid salinities for orpiment and calcite are 1.7 to 5.4 wt percent NaCl equiv, relative to 1.1 to 2.9 wt percent NaCl equiv for barite and realgar. The lower T_h and salinity for fluid inclusions in barite and realgar suggest fluid cooling and dilution, following the deposition of paragenetically earlier orpiment and calcite.

Introduction

One of the common characteristics of Carlin-type deposits from around the world, including Nevada, is a late-stage mineralizing event comprised of orpiment, realgar, pyrite, barite, calcite, and gold (Radtke et al., 1980; Cunningham et al., 1988; Turner et al., 1994). Complex intergrowths of late-stage minerals are common in Carlin-type deposits, but paragenetic relationships support a sequential and overlapping deposition for orpiment, calcite, realgar, and barite (Hofstra and Cline, 2000). The significance of this event in the genesis of Carlin-type deposits is somewhat obscured by fluid inclusion homogenization temperatures (T_h) in calcite, realgar, and barite that range from 77º to 342ºC (Radtke et al., 1980; Liu and Geng, 1985; Kuehn, 1989).

The purpose of this study is to determine if fluid inclusions have reequilibrated and to refine the temperature range at which the late-stage mineralization occurred. Fluid inclusion reequilibration is a significant issue and was addressed by documenting inclusion morphology, recording the behavior of inclusions during microthermometric analyses, measuring the gas content of inclusions in realgar and orpiment, and assessing conditions after inclusion entrapment. Large ranges in T_h could also reflect fluid boiling; therefore, point counts were conducted to document the different types of fluid inclusions in late-stage minerals.

Methods and Analysis

Samples from veins and breccias were obtained from the Betze and Carlin mines, Nevada. The location of these mines, in context with other Carlin-type deposits, is described in Hofstra and Cline (2000). Late-stage mineralization sampled in the JB faults (4,700 level), Betze mine, consists of open-space fillings of barite in silicified ores, and two discrete orpiment veins (e.g., veins 1 and 2) with calcite and realgar that crosscut jasperoid. At the bottom of the Carlin pit, late-stage mineralization is contained in a breccia with clasts of a silicified black shale and matrix of orpiment, calcite, and minor realgar. Samples were collected shortly after exposure in the pit, and then transported and stored in climate-controlled facilities.

Fluid inclusion microthermometric analyses were conducted on a Linkham T_h 600 heating and freezing stage. Individual crystals of barite and realgar were hand picked from samples and placed directly on the fluid inclusion stage for analysis. Sections of orpiment and calcite were cleaved from larger crystals using a razor blade. Due to the low hardness of late-stage minerals, the T_h of fluid inclusions was measured before freezing, which could cause stretching due to expansion associated with the formation of ice (Lawler and Crawford, 1983). Fluid inclusions in orpiment and calcite have T_h that could be repeated to within 1ºC. In contrast, fluid inclusions in barite and realgar commonly record progressively higher T_h with multiple heating runs. Decrepitation was a particular problem for fluid inclusions in orpiment and realgar, even starting with ramps of 5ºC per minute. When heating ramps of 30º to 40ºC per minute were used, it was not uncommon for realgar crystals to shatter. Salinities were determined by the freezing-point depression of aqueous inclusions (Bodnar, 1993). Ice formation in fluid inclusions hosted by realgar and barite commonly produced a visible expansion that caused some inclusions to rupture and produced microfractures around other inclusions, and, when ice melted in one-phase liquid inclusions, a vapor bubble frequently nucleated.

† Corresponding author: email, jagroff@email.msn.com

Fluid inclusion volatiles were released by in vacuo crushing at room temperature with the liberated gases measured directly by a quadrupole mass spectrometer (Norman and Musgrave, 1994). A binocular microscope was used to ensure the purity of two separates of realgar and orpiment from the JB faults, Betze mine. Both mineral separates were prepared using HCl and distilled water before being placed under vacuum for 12 h prior to analysis.

Results

Three types of fluid inclusions were identified in late-stage minerals. Negative crystal shapes characterize type 1 inclusions, which are one-phase liquid water and the dominant population of primary and secondary inclusions in realgar and barite (Fig. 1a; Table 1). Type 2 inclusions are two-phase, vapor-poor (<20% vapor), and are most abundant in orpiment and calcite (Fig. 1b; Table 1). These inclusions are generally rounded in calcite and elongate to angular in orpiment (Fig. 1b, c). Fluid inclusion types 1 and 2 are commonly small (e.g., 4–10 υm) in orpiment and calcite, relative to typical inclusions (e.g., 10–40 υm) in barite and realgar. Two-phase, vapor-rich (>50% vapor) fluid inclusions comprise type 3 and are common as secondary inclusions in calcite and orpiment vein #2 (Fig. 1c), and primary inclusions in orpiment vein #1 (Table 1). Fluid inclusions in various stages of necking down to produce types 1 to 3 were frequently observed in barite (Fig. 1d). No CO_2-rich fluid inclusions were identified in any samples at room temperature, and no clathrates were identified during freezing runs. Quadrupole mass spectrometer analyses confirm the gas-poor nature of late-stage mineralizing fluids at the Betze mine with total gas contents of 0.1 mole percent for realgar and 0.9 to 2.5 mole percent for orpiment (Table 2). The dominant gas species are CO_2 and N_2, with concentrations up to 1.1 and 1.4 mole percent, respectively (Table 2).

Fluid inclusions in barite suitable for microthermometric analysis were difficult to find, due to the frequency of inclusions in various stages of necking down, which produced inclusion types 1 to 3. Homogenization temperatures of 154° to 300°C were measured for type 2 inclusions that stretched during analysis and/or had phase ratios with >20 percent vapor (Fig. 2a; Table 3). In contrast, some type 2 inclusions

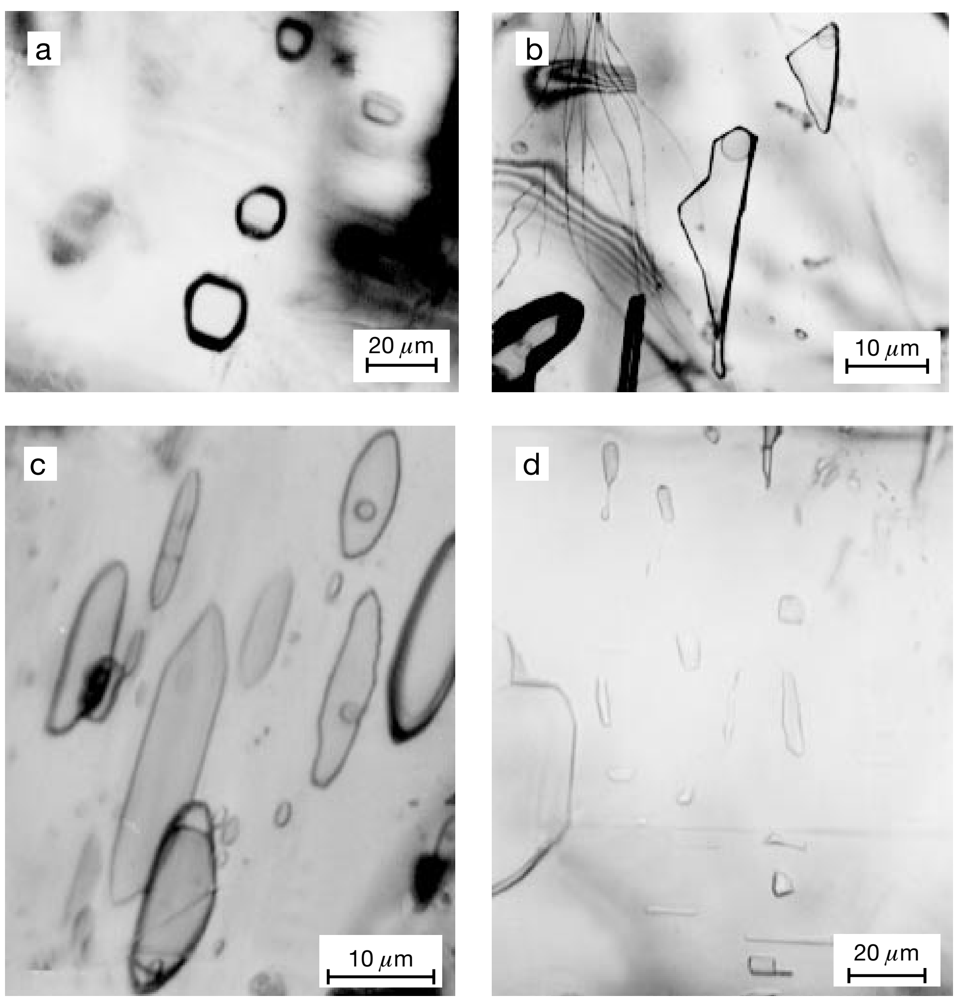

FIG. 1. Photomicrographs for samples from the Betze mine of (a) primary type 1 inclusions in realgar, (b) primary type 2 inclusions in orpiment vein 2, (c) secondary type 1, 2, and 3 (>50% vapor to left of scale or one-phase vapor with thick boundaries in upper right) inclusions in orpiment vein 2, and (d) primary type 1 inclusions in barite with tails and in the process of necking down (upper left).

TABLE 1. Point-Count Data for Primary and Secondary Fluid Inclusions in Orpiment, Realgar, Calcite, and Barite from the Betze and Carlin Mines

Host Mineral	Mine	Type 1 (%)	Type 2 (%)	Type 3 (%)	Number counted	Comments
Orpiment	Betze	10	55	35	250	Vein 1
Orpiment	Betze	5	95	0	80[1]	Vein 1
Orpiment	Betze	10	90	0	60	Vein 2
Orpiment	Betze	19	49	32	100[1]	Vein 2
Realgar	Betze	98	2	0	100	Vein 1
Barite	Betze	90	7	3	583	
Calcite	Betze	70	30	0	150	Vein 1
Calcite	Betze	0	10	90	50[1]	Vein 1
Calcite	Betze	15	85	0	70[1]	Vein 1
Calcite	Carlin	20	80	0	120	

[1]Indicates secondary fluid inclusions

TABLE 2. Quadrupole Mass Spectrometer Gas Data (mole %) for Fluid Inclusions in Orpiment and Realgar from the Betze Mine

Total gas	CH_4	N_2	CO_2
	Realgar		
0.1	<0.1	<0.1	<0.1
0.1	<0.1	<0.1	0.1
0.1	<0.1	<0.1	0.1
0.1	<0.1	<0.1	0.1
0.1	<0.1	<0.1	0.1
0.1	<0.1	<0.1	<0.1
	Orpiment		
2.1	<0.1	0.9	1.1
2.5	<0.1	1.4	1.0
2.2	<0.1	1.2	0.9
1.7	<0.1	0.7	0.9
2.3	<0.1	1.2	1.0
1.7	<0.1	0.8	0.9
1.3	<0.1	0.5	0.7
0.9	<0.1	0.3	0.6

with consistent phase ratios (e.g., 10% vapor) have repeatable T_h of 110° to 136°C (Fig. 2a; Table 3). Salinities for inclusion types 1 and 2 range from 2.1 to 2.6 wt percent NaCl equiv (Table 3).

Microthermometric analyses for realgar were complicated due to problems with the reequilibration (e.g., stretching and decrepitation) of fluid inclusions. A small number of type 2 inclusions have repeatable T_h of 100° to 137°C (Fig. 2b; Table 3). However, the majority of type 2 inclusions either decrepitated prior to homogenization or recorded progressively higher T_h, up to 250°C, with repeated heating runs (Fig. 2b; Table 3). Salinities for inclusion types 1 and 2 range from 1.2 to 1.6 and 1.1 to 2.9 wt percent NaCl equiv, respectively (Table 3).

Orpiment and calcite are closely associated and occur as intergrowths or as crystals of orpiment rimmed by calcite. Primary and secondary type 2 inclusions in calcite from the Carlin mine have T_h of 115° to 152°C and 113° to 135°C, respectively (Table 3). Orpiment from the Carlin mine contains primary and secondary type 2 inclusions that have T_h of 83° to 144°C and 101° to 157°C, respectively (Table 3). Salinities for primary

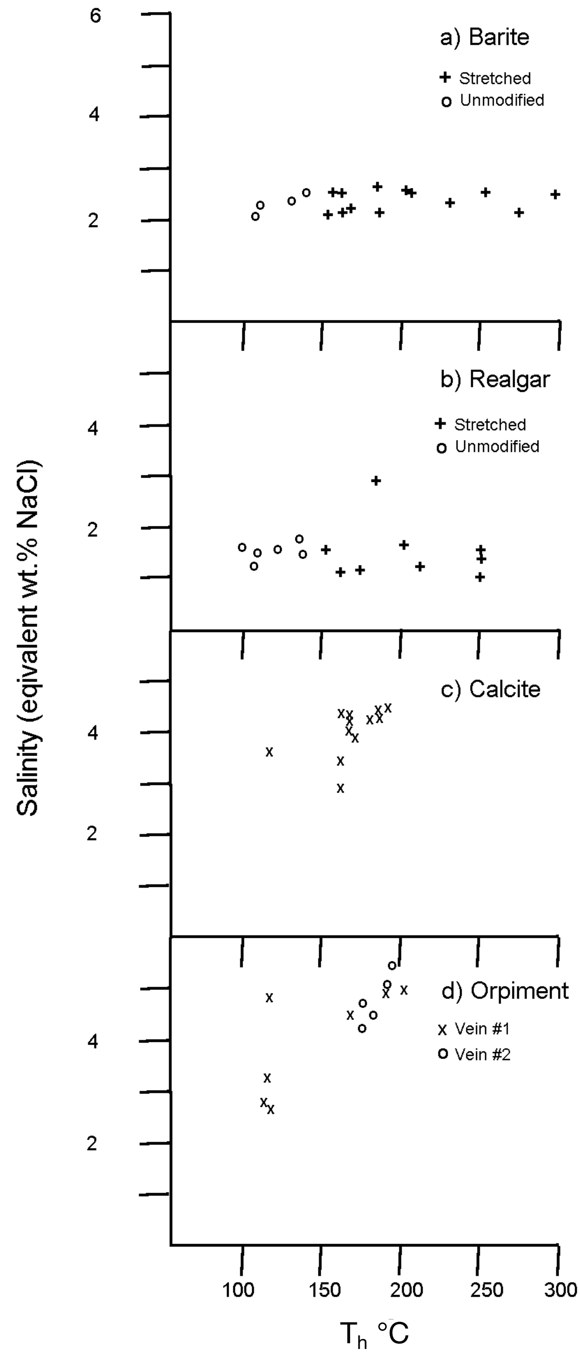

FIG. 2. Salinity versus T_h diagrams for primary fluid inclusions in (a) barite, (b) realgar, (c) calcite, and (d) orpiment from the Betze mine.

type 2 inclusions in orpiment range from 1.7 to 4.3 wt percent NaCl equiv (Table 3).

Higher T_h were measured for inclusion types 2 and 3 in samples of orpiment and calcite from the Betze mine. Primary and secondary type 2 inclusions in calcite have T_h of 122° to 191°C and 150° to 180°C, respectively (Fig. 2c; Table 3). Secondary type 3 inclusions occur in trails, but problems with decrepitation and poor optics prohibited the measurement of T_h or ice melting. Primary type 2 inclusions are the dominant population in orpiment vein 2 (Table 1), with T_h of

TABLE 3. A Compilation of Fluid Inclusion Data for Samples of Orpiment, Realgar, Calcite, and Barite from Select Carlin-Type Deposits

Host mineral	Mine	Inclusion type	Generation	Th (°C)	Avg	Mode of Th	Inclusions measured	Salinity	Avg	Inclusions measured	Comments
Orpiment	Betze	2	Primary	101–203	142	L	16	2.7–5.0	3.8	6	Vein 1
Orpiment	Betze	3	Primary	173, 189	181	V	2	NM	NA	NA	Vein 1
Orpiment	Betze	2	Primary	171–196	182	L	19	4.2–5.4	4.7	6	Vein 2
Orpiment	Betze	2	Secondary	200–212	207	L	13	3.2–4.0	3.7	3	Train 1
Orpiment	Betze	2	Secondary	102–165	134	L	9	5.3–5.7	5.6	6	Train 2
Orpiment	Betze	2	Secondary	NM	NA	NA	NA	4.5–5.3	4.8	10	Train 3
Orpiment	Carlin	2	Primary	83–144	108	L	32	1.7–4.3	3.1	4	Breccia
Orpiment	Carlin	2	Secondary	101–124	109	L	9	NM	NA	NA	Train 1
Orpiment	Carlin	2	Secondary	130–157	140	L	3	NM	NA	NA	Train 2
Calcite	Betze	2	Primary	122–191	166	L	23	2.9–4.5	4.1	23	Vein 1
Calcite	Betze	2	Secondary	150–171	172	L	22	3.7–4.0	3.9	20	Train 1
Calcite	Betze	2	Secondary	153–180	163	L	8	3.9–4.0	3.9	11	Train 2
Calcite	Carlin	2	Primary	115–152	137	L	20	NM	NA	NA	Breccia
Calcite	Carlin	2	Secondary	113–135	127	L	5	NM	NA	NA	Train 1
Calcite	Carlin	2	Secondary	114	114	L	2	NM	NA	NA	Train 2
Calcite	Carlin	2	Primary	106–143	126	L	8	0.2–2.3	1.5	8	Kuehn (1989)
Calcite	Carlin	2	Primary	121–213	172	L	4	0.2–0.7	0.5	4	Kuehn (1989)
Calcite	Carlin	1	Primary	170–218	193	L	23	2.0–4.0	3.0	23	Radtke et al. (1980)
Calcite	Messel	2	Primary	152–157	NR	L	NR	NR	NR	NR	Turner et al. (1994)
Calcite	Erzaiti	2	Primary	162–218	NR	L	NR	NR	NR	NR	Liu and Geng (1985)
Barite	Betze	1	Primary	NM	NA	NA	NA	2.1–2.6	2.4	4	Open-space filling
Barite	Betze	2	Primary	110–136	123	L	4	2.2–2.6	2.4	5	Open-space filling
Barite	Betze	2	Primary	154–300	196	L	16	2.1–2.6	2.5	13	Stretched
Barite	Carlin	2	Primary	77–219	148	L	14	0–1.7	0.9	14	Kuehn (1989)
Barite	Carlin	2	Primary	99–173	138	L	20	0.2–1.7	0.7	20	Kuehn (1989)
Barite	Carlin	2	Primary	106–198	133	L	9	0.3–2.5	0.7	9	Kuehn (1989)
Barite	Carlin	1	Primary	192–298	268	L	29	11.3–17.4	15.1	29	Radtke et al. (1980)
Barite	Carlin	2	Primary	235–342	290	L	12	NM	NA	NA	Radtke et al. (1980)
Barite	Carlin	2	Primary	260–340	326	L	20	NM	NA	NA	Radtke et al. (1980)
Barite	Carlin	2	Primary	229–304	273	L	12	<1	<1	12	Radtke et al. (1980)
Barite	Erzaiti	2	Primary	112–158	NR	L	NR	NR	NR	NR	Liu and Geng (1985)
Barite	Erzaiti	2	Primary	159–240	NR	L	NR	NR	NR	NR	Liu and Geng (1985)
Barite	Erzaiti	2	Primary	270–280	NR	L	NR	NR	NR	NR	Liu and Geng (1985)
Realgar	Betze	1	Primary	NM	NA	NA	NA	1.2–1.6	1.5	5	Vein 1
Realgar	Betze	2	Primary	100–137	119	L	8	1.2–1.6	1.4	6	Vein 1
Realgar	Betze	2	Primary	144–250	187	L	16	1.1–2.9	1.5	9	Stretched
Realgar	Carlin	1	Primary	~180–210	~205	L	14	NM	NA	NA	Radtke et al. (1980)
Realgar	Carlin	1	Primary	~200–>210	>210	L	21	NM	NA	NA	Radtke et al. (1980)

Abbreviations: L = liquid, NA = not analyzed, NM = not measured, NR = not reported, T_h = Homogenization temperature, V = vapor

171° to 196°C (Fig. 2d; Table 3). In contrast, orpiment vein 1 contains a large population of primary type 3 inclusions. Two of these inclusions had irregular shapes with narrow arms that allowed T_h of 173° and 189°C to be measured, but ice was not observed during freezing runs. Primary type 2 inclusions in this sample have T_h of 101° to 203°C (Fig. 2d; Table 3). Secondary trails of type 2 inclusions in orpiment veins have repeatable T_h of 102° to 165°C and 200° to 212°C (Table 3). Primary and secondary fluid inclusions in orpiment commonly decrepitate when T_h are exceeded by 30° to 40°C. Salinities for type 2 inclusions range from 2.9 to 4.5 and 2.7 to 5.7 wt percent NaCl equiv in calcite and orpiment, respectively (Table 3).

Discussion

P-T-t history

The interpretation of fluid inclusion data for barite, realgar, orpiment, and calcite is complicated by the potential reequilibration of inclusions. Investigations using synthetic fluid inclusions in quartz (Sterner and Bodnar, 1989; Vityk and Bodnar, 1995; Vityk and Bodnar, 1998) have determined that postentrapment P-T changes can cause overpressure or underpressure conditions to develop in inclusions, which lead to reequilibration through different mechanisms (e.g., stretching, decrepitation, or leakage). Some of the factors that determine whether reequilibration will occur include the size and shape of an inclusion, and the physical properties of the host mineral. Large fluid inclusions in quartz are the first to reequilibrate because they are surrounded by a high number of dislocation microstructures as documented by TEM images (Vityk et al., 2000). Irregularly shaped fluid inclusions generally reequilibrate before regularly shaped fluid inclusions in quartz based on studies by Bodnar et al (1989). Distinct changes in fluid inclusion morphology also accompany reequilibration with negative crystal shapes and "implosion haloes" produced by overpressure and underpressure conditions, respectively (Sterner and Bodnar, 1989).

Fluid inclusion studies are generally performed on minerals (e.g., quartz, calcite, and fluorite) that have very different physical properties. Therefore, under the same P-T conditions, fluid inclusions in cleavable soft minerals will reequilibrate before inclusions hosted by harder minerals, such as quartz. Heating tests by Ulrich and Bodnar (1988) document that fluid inclusions in barite, fluorite, and quartz begin to stretch when overheated by <10°, 20° to 30°, and >100°C, respectively. Due to the low hardness (e.g., 1.5 to 3.5) of late-stage minerals in Carlin-type deposits, reequilibration could occur during sample preparation or microthermometric analyses, as well as by geological processes that produced sufficient changes in P-T conditions after the trapping of fluid inclusions.

Age dating and geological relationships support the association of late-stage mineralization with Eocene volcanism and shallow-level igneous intrusions (Henry and Ressel, 2000; Hofstra and Cline, 2000). Late-stage mineralization at the Rodeo deposit has been dated at 39.7 Ma using the Rb-Sr method for galkhaite (Tretbar et al., 2000). The K/Ar age of 25.9 Ma for supergene alunite, with a $\delta^{34}S$ signature the same as primary sulfides in ore, from the Gold Quarry deposit (Arehart et al., 1992) suggests that late-stage mineralization along the Carlin trend may have been exposed at the surface within 14 m.y. of formation. This short interval of time would make it unlikely that late-stage minerals were deeply buried and then rapidly exhumed.

A shallow depth of formation is suggested by ore textures (e.g., brecciation and open-space fillings), the geochemistry of late-stage mineralization (e.g., As-Sb-Hg-Tl), and the gas-poor nature of fluid inclusions. No CO_2-rich fluid inclusions were identified in any late-stage minerals during this study or by Kuehn (1989) and Groff (1996). Quadrupole mass spectrometer crushing analyses also document low total gas contents for fluid inclusions in realgar and orpiment from the Betze mine (Table 2). Based on the behavior of vapor bubbles during crushing tests, Kuehn (1989) found no evidence for high-density, gas-rich fluid inclusions in late-stage minerals including a few quartz separates. This is in contrast to crushing tests that show positive evidence for high-density, gas-rich fluid inclusions in barite and calcite that predate Carlin-type mineralization, and in main-stage quartz (Kuehn, 1989). Similar relationships have been documented for the Twin Creeks mine, where a depth of approximately 1 km was calculated using gas data produced from quadrupole mass spectrometer crushing analyses for fluid inclusions in quartz intergrown with 42-Ma adularia (Groff, 1996).

Evidence for thermal events after late-stage mineralization at the Betze and Carlin mines is limited to the occurrence of travertine and calcite (Radtke et al., 1980; Kuehn, 1989). Fluid inclusions in travertine are all one-phase liquid water, which suggests a temperature of formation of ~100°C (Kuehn, 1989). Calcite interlayered with travertine from the Getchell mine contains liquid-rich, vapor-poor fluid inclusions that have T_h of 64° to 107°C and salinity 0.9 to 1.1 wt percent NaCl equiv (Groff, 1996). These low-temperature hydrothermal events, an absence of high concentrations of gases in fluid inclusions, the shallow depth of formation for late-stage mineralization, and a lack of evidence for burial and decompression suggest that fluid inclusions should still record trapping conditions. Late-stage minerals are also recognized as delicate open-space fillings, which would preclude the reequilibration of fluid inclusions as a result of thermal or mechanical stress related to the reactivation of fault zones.

Temperature range for late-stage mineralizing fluids

Orpiment and calcite at the Betze and Carlin mines are commonly intergrown, and both minerals host large populations of type 2 inclusions. Negative crystal shapes were not recognized and most fluid inclusions are small with round to elongate morphologies. These fluid inclusion characteristics, the use of cleaved sections for microthermometric analyses, the repeatability of T_h, and the P-T-t history discussed above provide strong evidence that inclusions in orpiment and calcite have not reequilibrated as a result of geological processes or during microthermometric analyses. Therefore, the best estimate of trapping conditions is provided by average T_h values of 142° to 182°C and 108° to 137°C for the Betze and Carlin mines, respectively. These values for T_h also overlap with data for calcite reported by other workers (Table 3).

Fluid inclusions in realgar and barite from the Betze mine are dominantly type 1 with a minor population of type 2 inclusions, and have the highest T_h for late-stage minerals (Table 3). Type 1 inclusions would have formed under low-temperature (~100°C) trapping conditions because there was not enough contraction of the fluid during cooling to form a vapor bubble (Roedder, 1984). High T_h were recorded for type 2 inclusions that reequilibrated by stretching during microthermometric analyses (Table 3). The necking down of fluid inclusions in barite from the Betze mine also produced type 2 inclusions with variable phase ratios and T_h. Reequilibration caused by geological processes that produced internal overpressure could be suggested by inclusions with negative crystal shapes in realgar and barite. However, fluid inclusions in realgar from the Betze mine are gas poor (Table 2), there is no geologic evidence to suggest a deep-seated origin followed by decompression, and the low temperature of younger hydrothermal events would not have caused inclusions in barite and realgar to overheat and stretch. Therefore, the best estimate of conditions during realgar and barite mineralization at the Betze mine is provided by temperature constraints imposed by type 1 inclusions and the lowest T_h of 100° to 110°C for type 2 inclusions (Table 3).

Estimated temperatures of 200° to 300°C for realgar and barite mineralization at the Carlin (Radtke et al., 1980; Kuehn, 1989) and Erzaiti (Liu and Geng, 1985) mines could reflect significantly hotter ore fluids or the reequilibration of fluid inclusions. High-temperature ore fluids are not supported by a fluid inclusion assemblage with a large component of one-phase liquid-water inclusions (Liu and Geng, 1985; Kuehn, 1989). Temperatures up to 300°C are also problematic because barite occurs near the end of the paragenesis for late-stage mineralization. If late-stage mineralization in Carlin-type deposits occurred at depths of ~1 km (Groff, 1996) and minerals were deposited along fractures open to the surface, then the confining pressure on fluid inclusions in paragenetically early orpiment and calcite would have been very low. Under these conditions, at the Carlin mine, the overheating of fluid inclusions in orpiment by 150° to 200°C would have resulted in high internal pressures accompanied by mass decrepitation, based on the experimental results of Tugarinov and Naumov (1970). Large numbers of decrepitated fluid inclusions were not observed in orpiment during this study or by Kuehn (1989). The high T_h for barite and realgar could be a result of reequilibration during microthermometric analyses, as documented at the Betze mine (this study) and/or the heating and other stresses caused by the production of doubly polished sections. The absence of vapor-rich fluid inclusions also precludes fluid boiling as a cause of ranges in T_h up to 140°C for individual samples of barite (Table 3). Therefore, the lowest T_h of 77° to 112°C for the Carlin and Erzaiti mines (Table 3) provide the best estimate of trapping conditions.

Paragenetic relationships support the deposition of orpiment and calcite followed by realgar and barite (Hofstra and Cline, 2000). The decrease in fluid inclusion T_h and salinities for orpiment and calcite versus paragenetically younger realgar and barite supports fluid cooling and dilution during late-stage mineralization.

Conclusions

The accurate interpretation of fluid inclusion data for late-stage mineralization at the Betze and Carlin mines is directly dependent upon the recognition of reequilibration. Factors such as the geological setting of the sample, fluid inclusion morphology, sample preparation techniques, and the physical properties of the host mineral were all considered in order to eliminate the possibility of fluid inclusion reequilibration in late-stage minerals prior to microthermometric analyses.

The reequilibration of some fluid inclusions during microthermometric analyses has resulted in an overestimation of fluid temperature during late-stage mineralization. Fluid inclusions hosted by realgar and barite were particularly susceptible to stretching during analyses, which resulted in large ranges in T_h. However, the dominance of type 1 inclusions and T_h as low as 100° to 110°C for type 2 inclusions support the deposition of barite and realgar at low temperatures. Type 2 inclusions in orpiment and calcite have repeatable T_h dominantly between 142° to 182°C and 108° to 137°C for the Betze and Carlin mines, respectively. The reequilibration of inclusions in orpiment and calcite produced by a younger thermal event or fault reactivation is not indicated, due to an absence of inclusions with negative crystal shapes or implosions haloes, the low temperature of travertine and calcite mineralization, and the pristine nature of delicate open-space fillings. Fluid salinities range from 1.7 to 5.4 wt percent NaCl equiv for orpiment and calcite, compared to 1.1 to 2.9 wt percent NaCl equiv for barite and realgar. Paragenetic relationships for these minerals document the deposition of orpiment and calcite prior to barite and realgar, which would allow for the cooling and dilution of fluids during late-stage mineralization.

Acknowledgments

We would like to thank Robert Bodnar for an insightful and thorough review of the manuscript. This project would not have been possible if not for the assistance of Keith Bettles, Barrick Goldstrike Mines, and Joseph Kowalick, Newmont Mining, with funding provided by the Charles Park Fellowship.

September 13, 2001; June 6, 2002

REFERENCES

Arehart, G.B., Kesler, S.E., O'Neil, J.R., and Foland, K.A., 1992, Evidence for the supergene origin of alunite in sediment-hosted micron gold deposits, Nevada: ECONOMIC GEOLOGY, v. 87, p. 263–270.

Bodnar, R.J., 1993, Revised equation and table for determining the freezing point depression of H_2O-NaCl solutions: Geochimica et Cosmochimica Acta, v. 57, p. 683–684.

Bodnar, R.J., Binns, P.R., and Hall, D.L., 1989, Synthetic fluid inclusions: VI. Quantitative evaluation of the decrepitation behaviour of fluid inclusions in quartz at one atmosphere confining pressure: Journal of Metamorphic Geology, v. 7, p. 229–242.

Cunningham, C.G., Ashley, R.P., Chou, I.M., Zushu, H., Chaoyuan, and Wenkand, L., 1988, Newly discovered sedimentary rock-hosted disseminated gold deposits in the People's Republic of China: ECONOMIC GEOLOGY., v. 83, p. 1462–1467.

Groff, J.A., 1996, $^{40}Ar/^{39}Ar$ geochronology of gold mineralization and origin of auriferous fluids for the Getchell and Twin Creeks mines, Humboldt County, Nevada: Unpublished Ph.D. thesis, Socorro, New Mexico Institute of Mining and Technology, 291 p.

Henry, C.D., and Ressel, M.W., 2000, Eocene magmatism of Northeastern Nevada: The smoking gun for Carlin-type gold deposits, *in* Cluer, J.K., Price, J.G., Struhsacker, E.M., Hardyman, R.F., and Morris, C.L., eds., Geology and ore deposits 2000: The Great basin and beyond: Geological Society of Nevada, Reno, Nevada, May 15–18, 2000, Symposium Proceedings, p. 365–388.

Hofstra, A.H., and Cline, J.S., 2000, Characteristics and models for Carlin-type gold deposits: Reviews in Economic Geology, v. 13, p. 163–220.

Kuehn, C.A., 1989, Studies of disseminated gold deposits near Carlin, Nevada: Evidence for a deep geologic setting of ore formation: Unpublished Ph.D. thesis, University Park, Pennsylvania State University, 384 p.

Lawler, J.P., and Crawford, M.L., 1983, Stretching of fluid inclusions resulting from a low-temperature microthermometric technique: ECONOMIC GEOLOGY, v. 78, p. 527–529.

Liu, D., and Geng, W., 1985, On the mineral association and mineralization conditions of the Carlin-type gold deposits in China: Geochimica et Cosmochimica Acta, v. 3, p. 277–282.

Norman, D.I., and Musgrave, J.A., 1994, N_2-Ar-He compositions in fluid inclusions: Indicators of fluid source: Geochimica et Cosmochimica Acta, v. 58, p. 1119–1131.

Radtke, A.S., Rye, R.O., and Dickinson, F.W., 1980, Geology and stable isotope studies of the Carlin gold deposit, Nevada: ECONOMIC GEOLOGY, v. 75, p. 641–672.

Roedder, E., 1984, Fluid Inclusions: Mineralogical Society of America Reviews in Mineralogy, v. 12, 646 p.

Sterner, S.M., and Bodnar, R.J., 1989, Synthetic fluid inclusions: VII. Reequilibration of fluid inclusions in quartz during laboratory-simulated metamorphic burial and uplift: Journal of Metamorphic Geology, v. 7, p. 243–260.

Tretbar, D.R., Arehart, G.B., and Christensen, J.N., 2000, Dating gold deposition in a Carlin-type deposit using Rb/Sr methods on the mineral galkhaite: Geology, v. 28, p. 947–950.

Tugarinov, A.I., and Naumov, V.B., 1970, Dependence of the decrepitation temperature of minerals on the composition of their gas-liquid inclusions and hardness: Akademia Nauk SSSR Doklady, v. 195, p. 112–114.

Turner, S.J., Flindell, P.A., Hendri, D., Hardjana, I., Lauricella, P.F., Lindsay, R.P., Marpaung, B., and White, G.P., 1994, Sediment-hosted gold mineralisation in the Ratatok district, north Sulawesi, Indonesia: Journal of Geochemical Exploration, v. 50, p. 317–336.

Ulrich, M.R., and Bodnar, R.J., 1988, Systematics of stretching of fluid inclusions II: Barite at 1 atm confining pressure: ECONOMIC GEOLOGY, v. 83, p. 1037–1046.

Vityk, M.O., and Bodnar, R.J., 1995, Do fluid inclusions in high-grade metamorphic terranes preserve peak metamorphic density during retrograde decompression?: American Mineralogist, v. 80, p. 641–644.

——1998, Statistical microthermometry of synthetic fluid inclusions in quartz during decompression reequilibration: Contributions to Mineralogy and Petrology, v. 132, p. 149–162.

Vityk, M.O., Bodnar, R.J., and Doukhan, J.C., 2000, Synthetic fluid inclusions: XV. TEM investigation of plastic flow associated with reequilibration of fluid inclusions in natural quartz: Contributions to Mineralogy and Petrology, v. 139, p. 285–297.